

Quadrupole interactions at divalent and trivalent europium sites in several europium oxides

Z. M. Stadnik

Ottawa-Carleton Institute of Physics, Department for Physics, University of Ottawa, Ottawa, Ontario, Canada K1N 6N5

G. Stroink

Department of Physics, Dalhousie University, Halifax, Nova Scotia, Canada B3H 3J5

T. Arakawa

Department of Industrial Chemistry, Kiniki University of Kyushu, Kayanomori, Iizuka, Fukuoka 820, Japan

(Received 14 March 1991; revised manuscript received 15 July 1991)

The electric-quadrupole interactions at the Eu sites in Eu_2CuO_4 , $\text{EuBa}_2\text{Cu}_3\text{O}_{7-x}$, $\text{Eu}_{0.6}\text{Sr}_{0.4}\text{VO}_{2.96}$, $\text{Eu}_3\text{V}_2\text{O}_7$, and Eu_2VO_4 have been studied at room temperature with ^{151}Eu Mössbauer spectroscopy. Whereas Eu ions are found to be in trivalent oxidation state in all these oxides, they also occur concurrently in the divalent state in $\text{Eu}_3\text{V}_2\text{O}_7$ and Eu_2VO_4 . It is found that the quadrupole coupling constant $eV_{zz}Q_g$ is negative in all oxides studied here and in the literature, except Eu_2CuO_4 . This is discussed in terms of different contributions to the electric-field-gradient tensor. The value $eV_{zz}Q_g = -18.032(134)$ mm/s found in Eu_2VO_4 is, to our knowledge, the largest ever reported for divalent Eu ions on any Eu oxide system.

I. INTRODUCTION

The most common oxidation state of europium in europium oxides is the trivalent one, with the $4f^65s^2 - ^7F_0$ electronic configuration. Europium also occurs in oxides in the divalent oxidation state, with the $4f^75s^2 - ^8S_{7/2}$ electronic configuration. These two oxidation states can be unambiguously determined by ^{151}Eu Mössbauer spectroscopy (MS). This is due to the different shielding of the closed shell s electrons by the $4f^6$ and $4f^7$ configurations, which results in an increase of the s -electron charge density at the center of the ^{151}Eu nucleus in Eu^{3+} oxides compared to the density in Eu^{2+} oxides.¹ This, in turn, induces a separation of about 14 mm/s between the Mössbauer absorption lines of divalent and trivalent europium atoms, which is much greater than the natural linewidth $\Gamma_{\text{nat}} = 1.31$ mm/s (Ref. 2), and thus easily detectable.

Eu atoms in various oxides are located at crystallographic sites with point symmetries which imply the existence of an electric field gradient (EFG) tensor.³ One can thus expect the presence of an electric quadrupole interaction between the EFG tensor and the known² electric quadrupole moment Q of the ^{151}Eu Mössbauer nucleus. This interaction should be manifested in ^{151}Eu Mössbauer spectra, especially in the paramagnetic ones. From fits of such spectra one can obtain the quadrupole coupling constant $eV_{zz}Q$, where V_{zz} is the principal component of the EFG tensor and e is the absolute value of the charge of the electron, and also the asymmetry parameter η .³ As opposed to widely used zero-field ^{57}Fe MS, ^{151}Eu MS provides information on both the absolute value and the sign of V_{zz} . This is very important since the knowledge of the experimental value of V_{zz} is essential for testing⁴ different theoretical models used to calcu-

late V_{zz} .⁵⁻⁷

For many oxides, $eV_{zz}Q$ is small and contributes to broadening of Eu^{3+} or Eu^{2+} lines in ^{151}Eu Mössbauer spectra. Such spectra are therefore fitted to a single Lorentzian line,⁸⁻¹⁷ from which the value of the isomer shift δ is extracted. Although one can unambiguously determine the oxidation state of Eu atoms from such fits because of the already mentioned large difference as compared to Γ_{nat} between the δ values of divalent and trivalent Eu ions, the valuable information on V_{zz} is lost. As has been shown in the literature,⁴ and as will be also demonstrated here, a careful analysis of paramagnetic ^{151}Eu Mössbauer spectra provides unambiguous information on the small value of $eV_{zz}Q$ and η . Furthermore, fits with a single Lorentzian line of unresolved quadrupole interaction give rise to errors in the values of δ .¹⁸ Although such errors are of no importance for distinguishing between Eu^{2+} and Eu^{3+} ions, they do hinder correct interpretation of small variations of δ within the same oxidation state in terms of variation of the electron charge density at the ^{151}Eu nucleus.

For most Eu oxides, Eu ions occur either as trivalent or divalent. However, for some oxides, divalent and trivalent ions are expected to be present concurrently. For example, based upon their chemical formulas, it is expected¹⁹ that both Eu^{2+} and Eu^{3+} ions exist in Eu_2VO_4 and $\text{Eu}_3\text{V}_2\text{O}_7$. There is, however, no direct experimental evidence to support this conjecture. It is the large difference between the δ values corresponding to Eu^{2+} and Eu^{3+} which makes ^{151}Eu MS an ideal tool to resolve such problems. Mixed metal niobates and tantalates of general formula $M_2^1M_2^2\text{Eu}_2M_{10}^3\text{O}_{30}$ ($M^1 = \text{Na, K}$; $M^2 = \text{Ca, Sr, Ba, Eu}$; $M^3 = \text{Nb, Ta}$), whose stoichiometry and magnetic properties were interpreted assuming the presence of only Eu^{2+} ions,²⁰ were shown^{12,13} by ^{151}Eu

MS to contain a substantial fraction of Eu^{3+} ions.

To elucidate the problem of the quadrupole interaction in oxides we present the results of ^{151}Eu MS study of a series of Eu oxides in which Eu atoms are located at crystallographic sites with nonzero values of V_{zz} . These results are compared with literature data and some general characteristics of the hyperfine parameters in oxides are found. The importance of various contributions to the EFG tensor is discussed and the experimental data are interpreted in terms of these contributions. Furthermore, we show that in Eu_2VO_4 and $\text{Eu}_3\text{V}_2\text{O}_7$ both divalent and trivalent Eu ions coexist. The electric quadrupole coupling constant of $-18.032(134)$ mm/s found in Eu_2VO_4 is, to our knowledge, the largest constant ever observed for Eu^{2+} ions in any oxide studied so far.

II. EXPERIMENTAL

The polycrystalline oxides of composition Eu_2VO_4 , $\text{Eu}_3\text{V}_2\text{O}_7$, Eu_2CuO_4 , and $\text{Eu}_{0.6}\text{Sr}_{0.4}\text{VO}_{2.96}$ were synthesized according to the procedure described in the literature.^{19,21,22} Eu_2O_3 , V_2O_3 , and V in the molecular ratios corresponding to Eu_2VO_4 and $\text{Eu}_3\text{V}_2\text{O}_7$ were mixed and ground. The mixture was pressed into pellets in a nitrogen stream; the pellets were then heated in vacuum using an induction furnace at 1723 K for 2 h. The Eu_2CuO_4 oxide was prepared from a mixture of dried Eu_2O_3 and CuO, and was fired at 1273 K in air for 20 h. A mixture of Eu_2O_3 , SrO and V_2O_3 corresponding to the $\text{Eu}_{0.6}\text{Sr}_{0.4}\text{VO}_{2.96}$ oxide was heated in vacuum at 1673 K for 1 h. All the samples were allowed to cool slowly to room temperature.

X-ray diffraction studies showed that the oxides were single phase. The first three oxides have a tetragonal crystal structure; and the fourth one, an orthorhombic structure, which is in agreement with the literature data.^{19,21-23}

Mössbauer measurements were conducted at room temperature using the 21.53-keV transition in ^{151}Eu . The Mössbauer spectra were recorded with a Wissel II spectrometer, which was calibrated with an iron foil.²⁴ A sinusoidal reference signal was used, resulting in two mirror-image spectra that were folded. A 100-mCi $^{151}\text{Sm}(\text{SmF}_3)$ source was used and the γ rays were detected with a proportional counter. The average surface densities of the four Mössbauer absorbers were respectively 19.6, 11.0, 16.3, and 11.9 mg Eu/cm². The absorbers can therefore be regarded as thin ones.²³

III. RESULTS AND DISCUSSION

A. Oxidation state of Eu atoms

A ^{151}Eu Mössbauer spectrum of Eu_2CuO_4 is shown in Fig. 1(a). At first glance it appears that the spectrum is a single line. However, an inspection of the fit with a single Lorentzian [Fig. 1(a)] shows that it does not properly describe the experimental spectrum. This is seen especially clearly in the difference spectrum [Fig. 1(b)] which exhibits structure resulting from the failure of the single

Lorentzian fit. Furthermore, the full linewidth at half maximum Γ found for Eu_2CuO_4 and other oxides (Table I) is significantly broader than the linewidth of about 2.0 mm/s expected for a thin absorber and the $^{151}\text{Sm}(\text{SmF}_3)$ source (broadening of the source line is due to the noncubic site at which ^{151}Sm nuclei are located in the SmF_3 matrix and to other factors inherent in source preparation).

The broadening of Γ obtained from single Lorentzian fits of Eu^{3+} lines of different oxides (Table I), which is much larger than that expected from a finite absorber thickness effect,²³ is evidence for the presence of a non-negligible quadrupole interaction. This interaction has been taken into account by fitting the ^{151}Eu Mössbauer spectra using a full Hamiltonian method. The ratio $R_Q = Q_e/Q_g$ of the excited and ground-state quadrupole moments was taken as 1.312.²

It is evident from Fig. 2(b) that the fit of the ^{151}Eu Mössbauer spectrum of Eu_2CuO_4 assuming a nonzero value of $eV_{zz}Q_g$ satisfactorily describes the shape of the experimental spectrum. This is also seen in the lack of any structure of the corresponding difference spectrum [Fig. 2(c)] and a much lower value of χ^2 as compared to the value corresponding to a single Lorentzian fit (Table

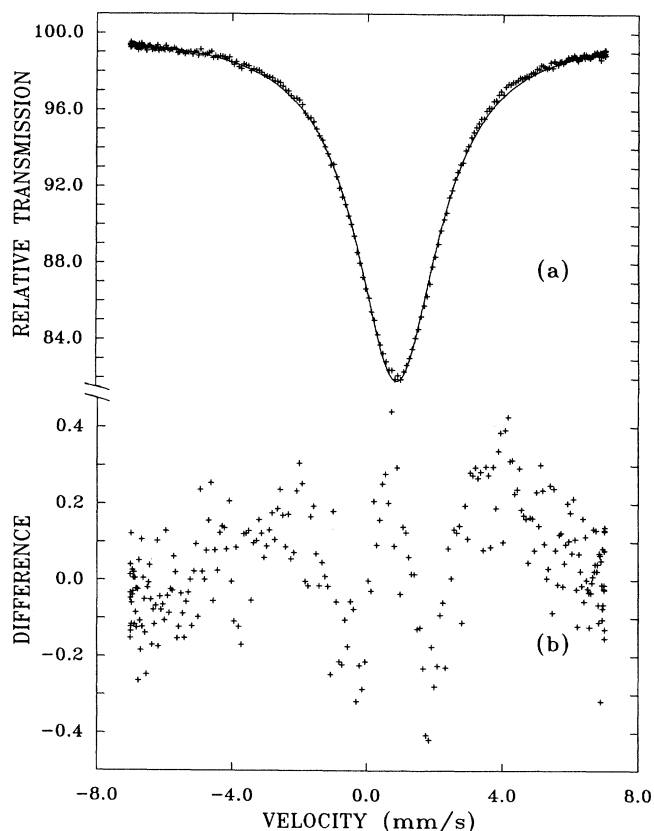


FIG. 1. (a) ^{151}Eu Mössbauer spectrum of Eu_2CuO_4 at room temperature. The solid line is a least-squares fit to a single Lorentzian. (b) Difference between the experimental and fitted spectra.

I). Furthermore, the value of Γ is now close to the value expected for a thin absorber. A similar observation can be made for other oxides studied here (Table I). For comparison, a ^{151}Eu Mössbauer spectrum of a high- T_c superconductor $\text{EuBa}_2\text{Cu}_3\text{O}_{7-x}$ studied previously,⁴ which has been now refitted using the exact Hamiltonian method, is shown in Fig. 2(a). The ^{151}Eu Mössbauer spectra of $\text{Eu}_{0.6}\text{Sr}_{0.4}\text{VO}_{2.96}$ and $\text{Eu}_3\text{V}_2\text{O}_7$ are shown in Figs. 3(a) and 3(b), respectively.

The δ value for Eu_2CuO_4 (Table I) proves that Eu ions are trivalent in this oxide. This agrees with the results of

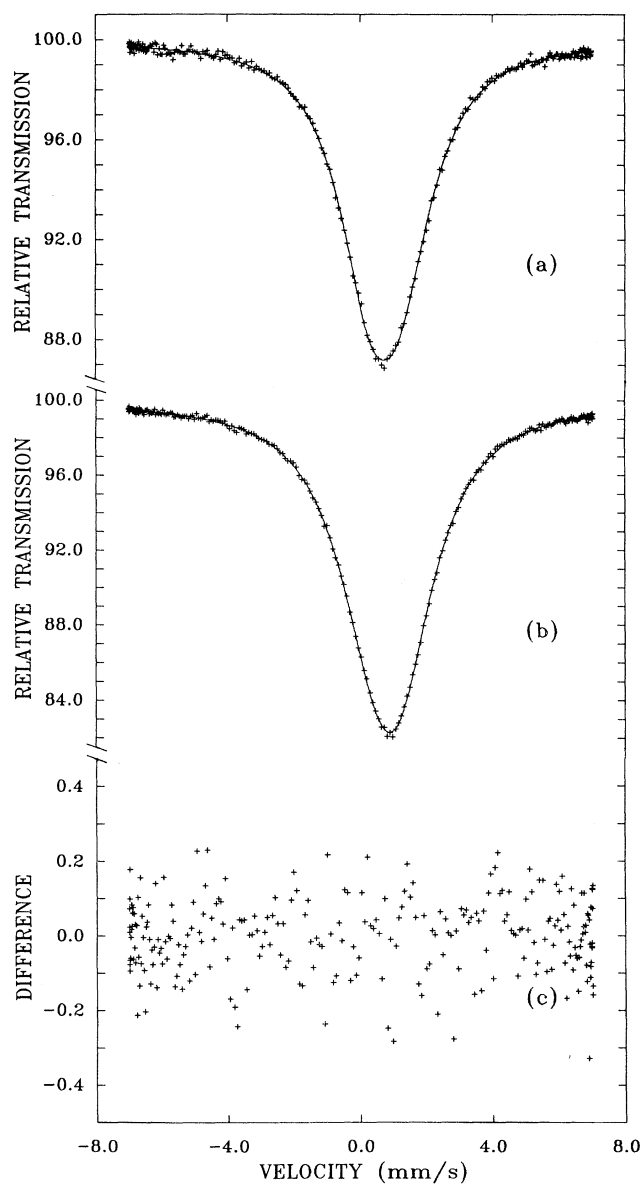


FIG. 2. Room-temperature ^{151}Eu Mössbauer spectra of (a) $\text{EuBa}_2\text{Cu}_3\text{O}_{7-x}$ and (b) Eu_2CuO_4 . The solid line is a least-squares fit assuming a nonzero quadrupole interaction. (c) Difference between the experimental and fitted spectra shown in (b).

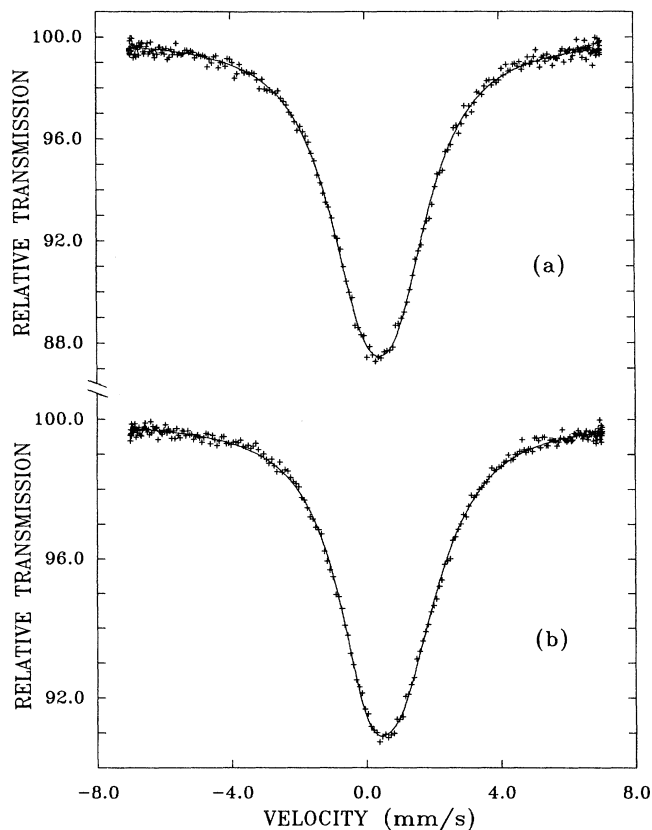


FIG. 3. Room-temperature ^{151}Eu Mössbauer spectra of (a) $\text{Eu}_{0.6}\text{Sr}_{0.4}\text{VO}_{2.96}$ and (b) $\text{Eu}_3\text{V}_2\text{O}_7$. The solid line is a least-squares fit assuming a nonzero quadrupole interaction.

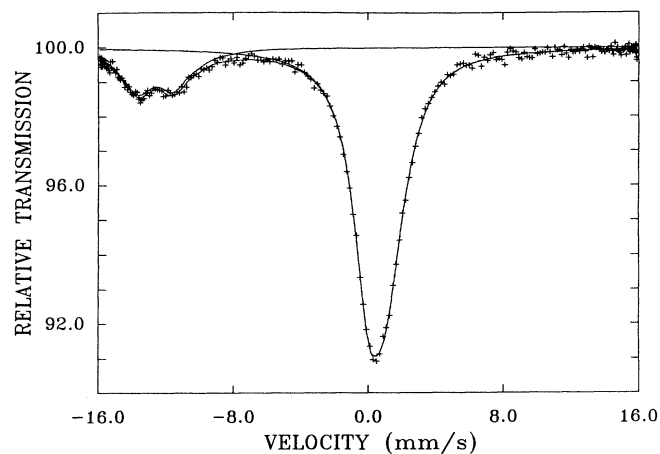


FIG. 4. ^{151}Eu Mössbauer spectrum of $\text{Eu}_3\text{V}_2\text{O}_7$ at room temperature. The solid line is a least-squares fit with two quadrupole subspectra, which are also shown, corresponding to divalent and trivalent Eu ions.

TABLE I. Room-temperature ^{151}Eu Mössbauer hyperfine parameters of oxides. The values of δ are given relative to the source. χ^2 is defined as $[\sum_{i=1}^k (y_i^{\text{expt}} - y_i^{\text{theor}})^2 / y_i^{\text{expt}}] / (k - m)$, where k and m are, respectively, the number of experimental points and the number of fitted parameters.

Oxide	δ (mm/s)	$eV_{zz}Q_g$ (mm/s)	η	Γ (mm/s)	χ^2
Eu_2CuO_4	0.866(2)	0 ^a		2.947(8)	2.55
	0.852(3)	4.482(123)	0.67(5)	2.529(26)	1.05
$\text{Eu}_{0.6}\text{Sr}_{0.4}\text{VO}_{2.96}$	0.410(5)	0 ^a		3.097(22)	1.80
	0.413(6)	5.817(106) ^b	1.00(6)	2.305(27)	1.12
$\text{EuBa}_2\text{Cu}_3\text{O}_{7-x}$	0.744(3)	0 ^a		2.758(11)	2.49
	0.761(5)	-5.348(120)	0.82(4)	2.093(32)	1.00
	0.795(5) ^c	0 ^{a,c}		2.805(21) ^c	1.91
$\text{Eu}_3\text{V}_2\text{O}_7$	0.828(6) ^c	-5.757(175) ^c	0.67(5) ^c	2.106(43) ^c	1.06
	0.589(5)	0 ^a		3.087(17)	2.35
	0.635(5)	-6.594(50)	0.60(6)	2.256(32)	1.02
Eu_2VO_4	-12.533(44)	-13.168(402)	0.81(8)	2.080(101)	1.01
	0.452(4)	0 ^a		3.588(16)	5.68
	0.536(5)	-8.043(65)	0.49(2)	2.445(22)	1.49
	-11.855(13)	-18.032(134)	0.25(2)	2.173(28)	1.24

^aValue fixed in the fit.

^bThe sign cannot be determined.

^cAbsorber at 4.2 K.

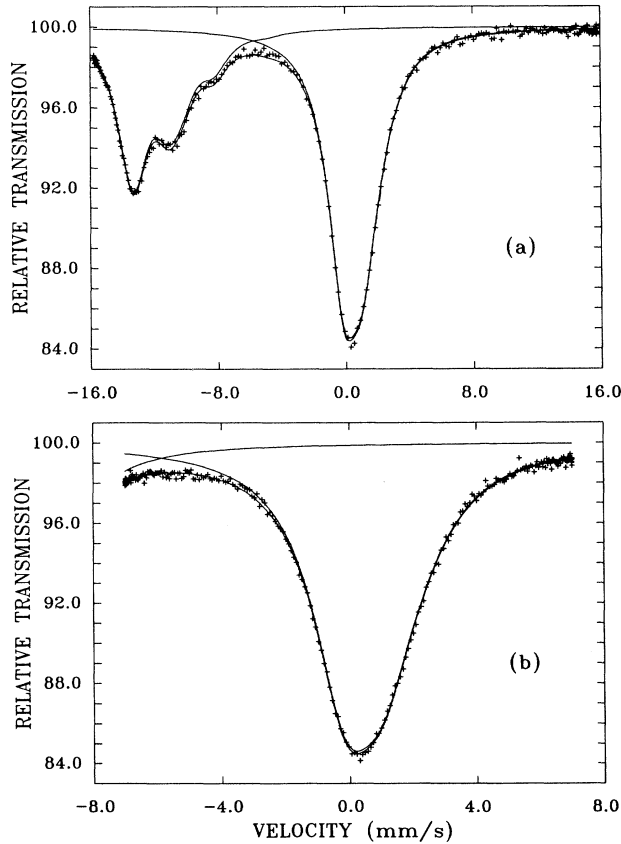


FIG. 5. Room-temperature ^{151}Eu Mössbauer spectra of Eu_2VO_4 measured for (a) large and (b) small velocity range. The solid line is a least-squares computer fit with two quadrupole subspectra, which are also shown, corresponding to divalent and trivalent Eu ions.

careful measurements and analysis of magnetic susceptibility of this oxide.²³ Similarly, Eu ions in $\text{Eu}_{0.6}\text{Sr}_{0.4}\text{VO}_{2.96}$ are trivalent (Table I), which is in agreement with susceptibility data.²⁵

It is evident from Fig. 3(b) and the value of δ (Table I) that Eu ions in $\text{Eu}_3\text{V}_2\text{O}_7$ are trivalent. However, as mentioned in the Introduction, one expects Eu atoms in this oxide to be present also in the divalent oxidation state. A ^{151}Eu Mössbauer spectrum of this oxide remeasured for a larger velocity range (Fig. 4) clearly shows the presence of Eu^{2+} ions with much larger magnitude of $eV_{zz}Q_g$ than that of Eu^{3+} ions (Table I). From the surface ratio of the Eu^{2+} and Eu^{3+} components of the spectrum, and assuming the same Debye-Waller factor for Eu^{2+} and Eu^{3+} ,^{2,3} we conclude that the fraction of the divalent Eu ions in $\text{Eu}_3\text{V}_2\text{O}_7$ is 17.1(8)%.

The ^{151}Eu Mössbauer spectrum of Eu_2VO_4 [Fig. 5(a)] clearly demonstrates the presence of both divalent and trivalent Eu ions. The magnitude of $eV_{zz}Q_g$ for Eu^{2+} is substantially larger than that for Eu^{3+} (Table I). The fraction of Eu^{2+} ions in this oxide is 39.0(1.6)%. To obtain a better resolution of the Eu^{3+} component of the ^{151}Eu Mössbauer spectrum, it was remeasured for a smaller velocity range [Fig. 5(b)].

B. Quadrupole interactions

It is clear from Table I that the values of χ^2 corresponding to the fits assuming $eV_{zz}Q_g \neq 0$ of Eu^{3+} lines of Mössbauer spectra of all oxides studied here are much smaller than the values corresponding to the fits with $eV_{zz}Q_g = 0$. Furthermore, the Γ values obtained from the quadrupole fits are consistent with the values expected for thin absorbers used in this study.²³ We thus conclude that there is a small electric quadrupole interaction at Eu^{3+} sites in all the oxides studied here.

The value of δ corresponding to Eu^{3+} ions increases for the following sequence of oxides (Table I): $\text{Eu}_{0.6}\text{Sr}_{0.4}\text{VO}_{2.96}$, Eu_2VO_4 , $\text{Eu}_3\text{V}_2\text{O}_7$, $\text{EuBa}_2\text{Cu}_3\text{O}_{7-x}$, and Eu_2CuO_4 . This means² that the s electron charge density at the Eu^{3+} nuclei increases for this sequence of oxides.

The quadrupole coupling constant $eV_{zz}Q_g$ at Eu^{3+} sites is negative for Eu_2VO_4 , $\text{Eu}_3\text{V}_2\text{O}_7$, and $\text{EuBa}_2\text{Cu}_3\text{O}_{7-x}$, and positive for Eu_2CuO_4 (Table I). Its sign cannot be determined for $\text{Eu}_{0.6}\text{Sr}_{0.4}\text{VO}_{2.96}$ since for $\eta=1.0$ (Table I) the transitions lie symmetrically spaced around the centroid of the Mössbauer spectrum.²⁶ For such a situation the true value of δ should coincide with the value obtained from a single Lorentzian fit,²⁶ which is indeed the case (Table I).

Two of the studied oxides, $\text{Eu}_3\text{V}_2\text{O}_7$ and Eu_2VO_4 , contain Eu atoms which are in trivalent and divalent oxidation states [Figs. 4 and 5(a), and Table I]. The more negative value of δ for Eu^{2+} in $\text{Eu}_3\text{V}_2\text{O}_7$ than in Eu_2VO_4 means a lower s electron charge density at Eu^{2+} nuclei in the former than in the latter.

Eu intermetallic compounds which contain Eu atoms in two oxidation states on crystallographically equivalent sites usually are in an intermediate valence state.²⁷ Their ¹⁵¹Eu Mössbauer spectra at low temperatures show Eu^{2+} and Eu^{3+} lines. At room temperature, however, these lines collapse to a single line whose value of δ is the weighted average of the δ values of Eu^{2+} and Eu^{3+} lines.²⁷ The fact that we observe at room temperature two distinct Eu^{2+} and Eu^{3+} lines [Figs. 4 and 5(a)] with δ values (Table I) characteristic for ionic Eu^{2+} and Eu^{3+} proves that these lines cannot be associated with a mixed valence phenomenon, which would be most unusual to occur in oxides. The individual integrity of Eu^{2+} and Eu^{3+} ions in $\text{Eu}_3\text{V}_2\text{O}_7$ and Eu_2VO_4 is thus puzzling. Its origin is unknown and should be studied theoretically. The only other Eu oxide system in which a similar integrity of the Eu^{2+} and Eu^{3+} ionic states was observed is the system of mixed metal niobates and tantalates.^{12,13}

The magnitude of the quadrupole coupling constant found at Eu^{2+} site in Eu_3VO_4 (Table I) is the largest reported to date for a divalent Eu ion in any oxide. A larger magnitude of this constant [$-19.289(289)$ mm/s] was found for trivalent Eu ions in $\text{Eu}_3\text{Ti}_2\text{O}_7$.²⁸ This can be compared with the value of $eV_{zz}Q_g$ (44–48 mm/s) reported for Eu^{2+} ions in stoichiometric and non-stoichiometric $\text{Eu}_x\text{Rh}_3\text{B}_3$,^{29,30} which is the largest ever reported for any Eu system.

In order to find out whether there are any common features of the quadrupole interaction at Eu sites in oxides, the literature values of $eV_{zz}Q_g$ and the ranges of the $eV_{zz}Q_g$ values for a given oxide series, measured in different oxides are presented in Table II. Two characteristics become evident. First, in most oxides of different crystal structure, except three cases^{32,43} discussed below, $eV_{zz}Q_g$ is negative both for divalent and trivalent Eu ions. Our results (Table I) support this general characteristic. The positive sign of $eV_{zz}Q_g$ found in a Eu-Sc-Fe garnet series³² may be due to the presence of some impurities in the samples.⁴⁶ Because of the small magnitude of $eV_{zz}Q_g$, and consequently a small departure of the spec-

trum from a single Lorentzian line shape, even a minute fraction of Eu-containing impurity can influence the sign of $eV_{zz}Q_g$. The presence of such an impurity is undoubtedly responsible for the positive sign of $eV_{zz}Q_g$ reported⁴³ for a high- T_c superconductor $\text{EuBa}_2\text{Cu}_3\text{O}_{7-x}$ (Table II). As was unambiguously shown in several studies^{4,42,44} (see also Table I), this sign is negative. As indicated above, the sign of $eV_{zz}Q_g$ for $\text{Eu}_{0.6}\text{Sr}_{0.4}\text{VO}_{2.96}$ could not be determined since $\eta=1.0$ (Table I).²⁶ The only oxide with positive $eV_{zz}Q_g$ is Eu_2CuO_4 , and possible reasons for this are discussed below. Second, the temperature change of magnitude of $eV_{zz}Q_g$ is small and negative^{4,28,35,42,43,45} (see also Table I) for temperatures below 300 K. However, for temperatures above 300 K, this change was reported to be small and positive.²⁸

Any component V_{ij} of the EFG tensor at an Eu nuclear site in an oxide may be written as⁴⁷

$$V_{ij} = V_{ij}^{(1)} + V_{ij}^{\text{latt}} + V_{ij}^{(2)}, \quad (1)$$

where $V_{ij}^{(k)}$ is due to the $4f$ configuration in k th order perturbation theory and V_{ij}^{latt} is the lattice contribution.

TABLE II. Room-temperature values of $eV_{zz}Q_g$ in trivalent and divalent Eu oxides and the range of $eV_{zz}Q_g$ values in oxide series.

Oxide	$eV_{zz}Q_g$ (mm/s)	Ref.
Trivalent Eu		
$\text{Eu}_3\text{Fe}_5\text{O}_{12}$	-13.82^a	31
$\text{Eu}_{3-y}\text{Sc}_{2+y}\text{Fe}_3\text{O}_{12}$	$4.24 \div 4.73^b$	32
$\text{Eu}_2\text{Ti}_2\text{O}_7$	-16.01	10
$\text{Eu}_2\text{Z}_2\text{O}_7$, $Z = \text{Ti, Ru, Ir, Mo, Sn, Zr, Pb, Pt, Hf}$	$-4.61 \div -19.29$	28
$\text{Eu}_2\text{SrFe}_2\text{O}_7$	-11.2^c	33
EuMO_3 , $M = \text{Cr, Mn, Fe, Co, Sc}$	$-5.59 \div -7.19$	34,35
$\text{EuFe}_{0.5}\text{Co}_{0.5}\text{O}_3$	-6.79	36
$\text{EuFe}_{0.5}\text{Cr}_{0.5}\text{O}_3$	-7.23	37
EuRO_3 , $R = \text{Gd, Dy, Ho, Er, Yb, Lu, Tm, Tb, Sm, Nd, Pr}$	$-4.83 \div -8.95$	38,39
$\text{EuCeO}_{3.5}$	-4.79	39
$\text{Eu}_{0.2}\text{R}_{0.8}\text{FeO}_3$, $R = \text{La, Sm, Gd, Tb, Dy, Ho, Er, Tm, Yb, Lu}$	$-6.02 \div -6.96$	40
$\text{EuFe}_{0.8}\text{M}_{0.2}\text{O}_3$, $M = \text{Sc, Cr, Mn, Co}$	$-6.94 \div -8.20$	40
$(\text{Eu}_x\text{Y}_{1-x})_{0.3}\text{Ba}_{0.7}\text{CuO}_3$	$-3.40 \div -7.40$	41
$\text{EuBa}_2\text{Cu}_3\text{O}_{7-x}$	-4.35	42
	-5.35^d	42
	5.9^d	43
	-4.46	44
Divalent Eu		
Eu_2TiO_4	-10.88	45
$\text{Eu}_3\text{Ti}_2\text{O}_7$	-9.21	45

^aAt 81 K.

^bAt 77 K.

^cAt 85 K.

^dAt 4.2 K.

The lattice contribution is due to the charge distribution of the surrounding ions in the crystal lattice. It does not depend on temperature if lattice expansion is negligible. For Eu^{3+} ions with the 7F_0 ground state, there is no first-order $4f$ contribution. However, since the excited states 7F_1 and 7F_2 lie relatively low above the ground state, there is a significant second-order $4f$ contribution to the EFG tensor, which is weakly temperature dependent. For Eu^{2+} ions with the ${}^8S_{7/2}$ ground state, the lattice term is the only appreciable contribution.

A compilation of literature calculations, based on a point-charge model, of the lattice contribution to $eV_{zz}Q_g$ for Eu^{3+} and Eu^{2+} in oxides of different crystal structures is presented in Table III. It is evident that, independent of crystal structure of an oxide, the lattice contribution is negative. Thus, the lattice contribution accounts for the negative sign of $eV_{zz}Q_g$ determined experimentally (Tables I and II). The point-charge model calculations for divalent Eu ions (Table III) account reasonably well for the order of magnitude of the experimental $eV_{zz}Q_g$ (Table II), in spite of limitations inherent to such calculations.^{4,49} For trivalent Eu ions, apart from the lattice contribution, one also has to calculate the second-order $4f$ contribution. Calculations of the latter, which are more complex, require information on crystal field parameters for a given oxide,^{33,34,48} which are often not available. Such calculations show^{33,34} that $eV_{zz}^{(2)}Q_g$ is positive and equal in magnitude to about half of $eV_{zz}^{\text{latt}}Q_g$.^{28,34} It may thus be concluded that in all oxides considered here (Tables I and II), except Eu_2CuO_4 (Table I), the experimentally determined negative sign of $eV_{zz}Q_g$ for trivalent Eu ions reflects the expected larger lattice contribution to the EFG tensor rather than of the second-order $4f$ contribution. The positive sign of $eV_{zz}Q_g$ in Eu_2CuO_4 is most probably due either to the stronger $eV_{zz}^{(2)}Q_g$ contribution than the $eV_{zz}^{\text{latt}}Q_g$ contribution, or to an additional positive contribution whose origin is unknown.

IV. SUMMARY

¹⁵¹Eu Mössbauer spectra of a series of Eu oxides were measured at room temperature. Their analysis shows that the sign of the electric quadrupole coupling constant

TABLE III. Calculated lattice contribution $eV_{zz}^{\text{latt}}Q_g$ for trivalent and divalent Eu ions in different oxides.

Oxide	$eV_{zz}^{\text{latt}}Q_g$ (mm/s)	Ref.
Trivalent Eu		
$\text{Eu}_2\text{Ti}_2\text{O}_7$	-21.33	28
$\text{Eu}_2\text{Pb}_2\text{O}_7$	-19.69	28
$\text{Eu}_2\text{SrFe}_2\text{O}_7$	-21.08	33
EuFeO_3	-15.06	34
EuSrFeO_4	-18.5	48
$\text{Eu}_{3-y}\text{Sc}_{2+y}\text{Fe}_3\text{O}_{12}$	-11.16 ÷ -12.56 ^a	32
	-8.41 ÷ -10.38 ^b	32
$\text{Eu}_3\text{Fe}_3\text{O}_{12}$	-11.25 ^a	49
	-11.00 ^b	
Divalent Eu		
Eu_2TiO_4	-7.54	45
$\text{Eu}_3\text{Ti}_2\text{O}_7$	-6.62	45

^aFor the dipole polarizability of oxygen $\alpha = 1.0 \text{ \AA}^3$.

^bFor $\alpha = 0.1 \text{ \AA}^3$.

$eV_{zz}Q_g$ at Eu^{2+} and Eu^{3+} sites is negative, except for Eu_2CuO_4 for which this constant is positive. The value $eV_{zz}Q_g = -18.032(134) \text{ mm/s}$ found for Eu^{2+} ions in Eu_2VO_4 is the largest reported to date for a divalent Eu ion in any oxide. Divalent and trivalent Eu ions are found to exist simultaneously at the same crystallographic sites in Eu_2VO_4 and $\text{Eu}_3\text{V}_2\text{O}_7$. The review of literature data on the measured values of $eV_{zz}Q_g$ shows that this constant is negative for all the oxides studied so far, except the oxide Eu_2CuO_4 . This general behavior is shown to be due to the predominant negative lattice contribution to the EFG tensor. It is also found that for trivalent Eu ions the magnitude of $eV_{zz}Q_g$ decreases with temperature.

ACKNOWLEDGMENTS

This work was supported by the Natural Sciences and Engineering Research Council of Canada.

¹E. R. Bauminger, G. M. Kalvius, and I. Nowik, in *Mössbauer Isomer Shifts*, edited by G. K. Shenoy and F. E. Wagner (North-Holland, Amsterdam, 1978), p. 661.

²J. G. Stevens, in *Handbook of Spectroscopy*, edited by J. W. Robinson (CRC, Boca Raton, Florida, 1981), Vol. III, p. 464.

³P. Gülich, R. Link, and A. Trautwein, in *Mössbauer Spectroscopy and Transition Metal Chemistry*, Inorganic Chemistry Concepts, Vol. 3, edited by M. Becke, Ch. K. Jørgensen, M. F. Lappert, S. J. Lippard, J. L. Margrave, K. Niedenzu, R. W. Parry, and H. Yamatera (Springer-Verlag, Berlin, 1978).

⁴Z. M. Stadnik, G. Stroink, and R. A. Dunlap, *Phys. Rev. B* **39**, 9108 (1989).

⁵F. J. Adrian, *Phys. Rev. B* **38**, 2426 (1988).

⁶S. Nagel, *J. Phys. C* **18**, 3673 (1985); *J. Phys. Chem. Solids* **46**, 743 (1985).

⁷P. Blaha, K. Schwartz, and P. Herzig, *Phys. Rev. Lett.* **54**, 1192 (1985).

⁸P. Brix, S. Hüfner, P. Kienle, and D. Quitmann, *Phys. Lett.* **13**, 140 (1964).

⁹G. Gerth, P. Kienle, and K. Luchner, *Phys. Lett.* **27A**, 557 (1968).

¹⁰G. W. Dulaney and A. F. Clifford, in *Mössbauer Effect Methodology*, edited by I. J. Gruverman (Plenum, New York, 1970), Vol. 5, p. 65.

¹¹V. G. Jadhao, R. M. Singru, G. N. Rao, D. Bahadur, and C. N. R. Rao, *J. Phys. Chem. Solids* **37**, 113 (1976).

- ¹²N. N. Greenwood, F. Viegas, and F. Studer, *J. Solid State Chem.* **31**, 347 (1980).
- ¹³F. Studer, G. Allais, and B. Raveau, *J. Phys. Chem Solids* **41**, 1187 (1980).
- ¹⁴J. M. D. Coey and K. Donnelly, *Z. Phys.* **67**, 513 (1987).
- ¹⁵M. Eibschütz, D. W. Murphy, S. Sunshine, L. G. Van Uitert, S. M. Zahurak, and W. H. Grodkiewicz, *Phys. Rev. B* **35**, 8714 (1987).
- ¹⁶J. Marcus, C. Escribe-Filippini, R. Chevalier, and R. Buder, *Solid State Commun.* **62**, 221 (1987).
- ¹⁷E. Kuzmann, Z. Homonnay, A. Vértes, M. Gál, K. Torkos, B. Csákvári, G. K. Solymos, G. Horváth, J. Bánkúti, I. Kirschner, and L. Korecz, *Phys. Rev. B* **39**, 328 (1989).
- ¹⁸B. A. Goodman, N. N. Greenwood, and G. E. Turner, *Chem. Phys. Lett.* **5**, 181 (1970).
- ¹⁹T. Shin-ike, H. Hata, T. Sakai, G. Adachi, and J. Shiokawa, *Mater. Res. Bull.* **11**, 1361 (1976).
- ²⁰F. Studer, J. P. Fayolle, and B. Raveau, *Mater. Res. Bull.* **11**, 1125 (1976).
- ²¹T. Arakawa, S. Takeda, G. Adachi, and J. Shiokawa, *Mater. Res. Bull.* **14**, 507 (1979).
- ²²T. Shin-ike, T. Sakai, G. Adachi, and J. Shiokawa, *Mater. Res. Bull.* **11**, 249 (1976).
- ²³M. Tovar, D. Rao, J. Barnett, S. B. Oseroff, J. D. Thompson, S. W. Cheong, Z. Fisk, D. C. Vier, and S. Schultz, *Phys. Rev. B* **39**, 2661 (1989).
- ²⁴*Certificate of Calibration, Iron Foil Mössbauer Standard*, edited by J. P. Cali, Natl. Bur. Stand. (U.S.) No. 1541 (U.S. GPO, Washington, DC, 1971).
- ²⁵T. Shin-ike, T. Sakai, G. Adachi, and J. Shiokawa, *Mater. Res. Bull.* **12**, 269 (1977).
- ²⁶A. L. Nichols, N. R. Large, and G. Lang, *Chem. Phys. Lett.* **15**, 598 (1972).
- ²⁷M. Croft, J. A. Hodges, E. Kemly, A. Krishnan, V. Murgai, and L. C. Gupta, *Phys. Rev. Lett.* **48**, 826 (1982).
- ²⁸C. L. Chien and A. W. Sleight, *Phys. Rev. B* **18**, 2031 (1978).
- ²⁹S. A. Shaheen, M. Abd-Elmeguid, H. Miklitz, J. S. Schilling, P. Klavins, and R. N. Shelton, *Phys. Rev. Lett.* **55**, 312 (1985).
- ³⁰S. K. Malik, G. K. Shenoy, S. M. Heald, and J. M. Tranquada, *Phys. Rev. Lett.* **55**, 316 (1985).
- ³¹I. Nowik and S. Ofer, *Phys. Rev.* **132**, 241 (1963).
- ³²Z. M. Stadnik and B. F. Otterloo, *J. Solid State Chem.* **48**, 133 (1983).
- ³³T. C. Gibb, *J. Phys. C* **14**, 1985 (1981).
- ³⁴T. C. Gibb, *J. Chem. Soc. Dalton Trans.* 2245 (1981).
- ³⁵Z. M. Stadnik and E. De Boer, *Solid State Commun.* **50**, 335 (1984).
- ³⁶T. C. Gibb, *J. Chem. Soc. Dalton Trans.* 873 (1983).
- ³⁷T. C. Gibb, *J. Chem. Soc. Dalton Trans.* 2031 (1983).
- ³⁸S. Wenhui, L. Xiaoxiang, J. Mingzhi, X. Weiming, W. Daiming, and L. Milan, *Phys. Rev. B* **37**, 35 (1988); J. Mingzhi, L. Xiaoxiang, S. Wenhui, X. Weiming, W. Daiming, and L. Milan, *Hyperfine Interact.* **40**, 303 (1988); Z. Xin, S. Wenhui, X. Weiming, L. Xiaoxiang, W. Daiming, and J. Mingzhi, *High Pressure Res.* **1**, 131 (1989).
- ³⁹S. Wenhui, X. Weiming, Z. Xin, L. Xiaoxiang, W. Daiming, and J. Mingzhi, *Phys. Rev. B* **40**, 102 (1989).
- ⁴⁰J. Mingzhi, L. Xuewu, Z. Weixing, S. Wenhui, X. Weiming, and L. Milan, *Solid State Commun.* **76**, 985 (1990).
- ⁴¹X. Weiming, L. Xiaoxiang, J. Mingzhi, H. Lanying, W. Yifeng, Z. Jianshi, L. Hongjian, L. Liping, and S. Wenhui, *Int. J. Mod. Phys. B* **1**, 325 (1987).
- ⁴²A. Freimuth, S. Blumenröder, G. Jackel, H. Kierspel, J. Langen, G. Buth, A. Nowack, H. Schmidt, W. Schlabit, and E. Zirngiebl, *Z. Phys. B* **68**, 433 (1987).
- ⁴³P. Vulliet, A. Yaouanc, G. M. Kalvius, R. Chaudouet, P. Bermis, R. Madar, A. Rouault, and J. P. Senateur, *Hyperfine Interact.* **42**, 1258 (1988).
- ⁴⁴M. Lippmaa, E. Realo, and K. Realo, *Phys. Lett. A* **139**, 353 (1989).
- ⁴⁵C. -L. Chien, S. DeBenedetti, and F. De S. Barros, *Phys. Rev. B* **10**, 3913 (1974).
- ⁴⁶Z. M. Stadnik and E. De Boer, *J. Phys. Chem. Solids* **45**, 113 (1984).
- ⁴⁷J. Blok and D. A. Shirley, *Phys. Rev.* **143**, 278 (1966).
- ⁴⁸F. Sevšek and D. Hanžel, *J. Phys. C* **16**, 6047 (1983).
- ⁴⁹Z. M. Stadnik, *J. Phys. Chem. Solids* **45**, 311 (1984).